A Low-Power Integrated Circuit for Interfacing a Capacitive Micromachined Ultrasonic Transducer (CMUT) Based Resonant Gas Sensor

M. Kumar, C. Seok, M. M. Mahmud, X. Zhang, and Ö. Oralkan
Department of Electrical and Computer Engineering
North Carolina State University
Raleigh, NC, USA
mohitk@ncsu.edu

***Abstract*—In this work we present a complete end-to-end interface for a capacitive micromachined ultrasonic transducer (CMUT) intended for low-power gas sensing applications. A prototype chip was designed in a 0.18-μm BiCMOS process. Different blocks (a BJT-based Colpitts oscillator, an inverter-based oscillator, a sine-to-square wave converter, a digital frequency counter, and a parallel-to-serial converter) required for the complete system are discussed, designed, and tested for their standalone performance. Consequently, a complete system interfaced with a 3.6-MHz CMUT and providing a digital frequency output is presented. With duty cycling for one measurement per minute the system consumed 10 μW power.**

***Keywords*—Low-power, CMUT interface, integrated circuit, digital output.**

I. Introduction

There has been an increase in the use of microelectromechanical systems (MEMS) based sensors for different applications because of their small form factor and low power consumption. Health and environmental tracking (HET) is one of the application areas utilizing MEMS technology. HET helps in understanding the effects of environmental pollutants on chronic diseases. There is thus a need for wearable systems, which can monitor the concentration of volatile organic compounds (VOCs) at very low power.

Capacitive micromachined ultrasonic transducers (CMUTs) operating as mass-loading sensors have emerged as a strong candidate for VOC detection. CMUTs are power efficient when compared with metal-oxide based resistive sensors, which generally require heating for their operation. In comparison to cantilever sensors, CMUTs have higher Q-factor for the same area of detection. Furthermore, SAW-based sensors have lower sensitivity and larger size, while FBAR-based sensors suffer from high-frequency noise limiting the minimum gas concentration that can be detected [1]. In addition, CMUTs also provide the advantage of implementing arrays of sensors on the same die, which could potentially improve selectivity, and enable differential sensing for removing offsets and long term frequency drifts.

In this paper we report a low-power end-to-end integrated interface for a CMUT gas sensor. The complete integrated system interfaced with a CMUT tracks changes in the parallel resonant frequency due to mass loading and provides a digital output.

The paper is organized as follows. Section II discusses the operating principle. Section III discusses the circuit implementation. Section IV presents measured results from the prototype chip.

Funding provided by National Science Foundation under Grant No. 1160483.

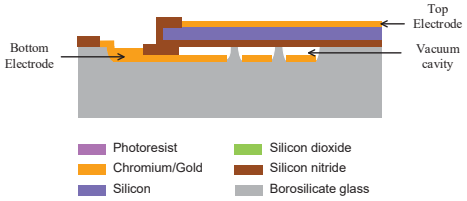

Fig. 1. Cross-section of the CMUT fabricated at the North Carolina State University Nanofabrication Facility by the Integrated Microsystems for Imaging, Sensing, and Therapy (iMIST) Lab [3].

II. Operating Principle

A. Resonant sensor

A CMUT is used as the resonant sensor for this work. CMUTs used in this study were fabricated using a three-mask anodic bonding process [2]. Fig. 1 shows the cross-sectional view of the fabricated CMUTs [3]. To achieve a high-Q resonant behavior, CMUTs are used under a specific DC bias, close to their pull-in voltage.

The electrical equivalent circuit model of a CMUT is represented by a four-element Butterworth-van-Dyke (BvD) model (Fig. 2), which has a series-RLC branch composed of R_E, L_E, and C_E, and C_O in parallel [4]. In the BvD model of the CMUT, C_O corresponds to the actual capacitance present due to parallel plate-structure. R_E represents the mechanical and radiation losses, L_E represents the mass, and C_E represents the stiffness of the thin plate.

B. Mass loading

For using the CMUT resonator as a gas sensor, the vibrating thin plate is coated with a very thin layer of polymer, which is selected so as to selectively adsorb the targeted gas present in the environment. Presence of the targeted gas in the environment will lead to adsorption of the gas molecules

978-1-4799-8203-5/15/$31.00 ©2015 IEEE

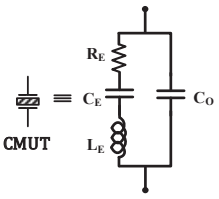

Fig. 2. Butterworth-van-Dyke (BvD) electrical equivalent circuit model of the CMUT [4].

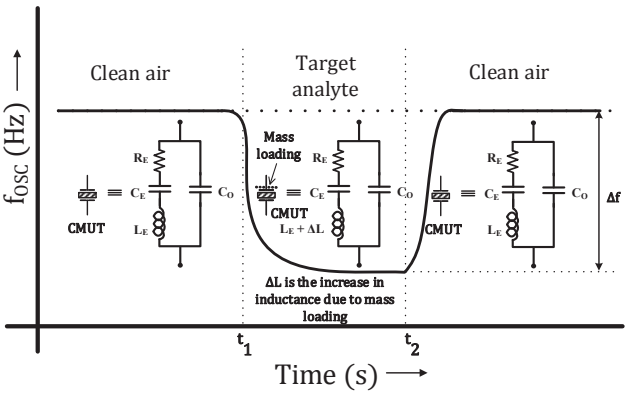

Fig. 3. Mass loading of the CMUT with target analyte, inductance in electrical equivalent model increases by ΔL when target analyte is present [1].

by the polymer, which increases the mass of the CMUT plate. Minimum concentration of the gas that can be detected depends on minimum detectable mass change (∂m). Equation 1 shows the relation between change in mass (∂m) and the frequency shift (∂f). From equation 1 it can be observed that for achieving minimum ∂m we need to operate at higher resonant frequency (f_0) and also we should be able to detect minimum frequency shift (∂f). f_0 is the design parameter for the CMUT and minimum detectable ∂f is limited by the noise of the sensor and the circuit.

$$\partial f = -\frac{1}{2} \cdot \frac{f_0}{m} \cdot \partial m \tag{1}$$

Fig. 3 shows the basic idea of mass loading. At time t_1 a certain concentration of targeted gas is passed through the environment, polymer adsorption leads to increase in the mass of the plate, which is equivalent to increase in the inductance (ΔL) in the CMUT electrical model. Due to this increase in inductance there will be a shift in the resonant frequency represented by Δf in Fig. 3. At time t_2 clean air is flowed over the gas sensor to remove the adsorbed particles from the polymer layer, and the original resonant frequency is restored.

C. Complete system overview

An electrical oscillator is interfaced with the CMUT to convert resonance in impedance into a sinusoidal signal. CMUTs are operated near their parallel resonant frequency, at which a higher quality factor can be achieved. For that reason generally a Colpitts architecture or an amplifier-based architecture is used [1]. The system presented here is intended as a wearable platform for detecting environmental pollutants, which are generally present in higher concentrations. So, sensitivity

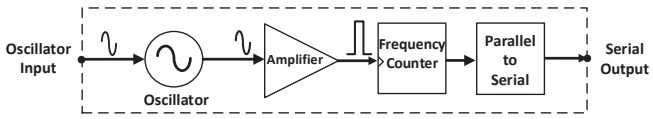

Fig. 4. Complete signal-flow from CMUT interface to final digital value [5].

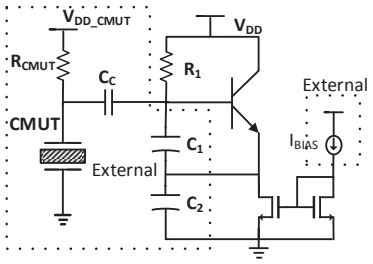

Fig. 5. BJT-Colpitts oscillator interfaced with CMUT [5].

required for the system is not extremely demanding compared to applications such as detection of chemicals warfare agents. However, total power consumption of the sensor should be very low ($<$100 μW) to meet the overall system power consumption budget. So, minimizing the power consumption is the main design constraint for the presented system. Fig. 4 shows the complete signal flow from interfacing the CMUT to the final digital output. The CMUT is interfaced with the oscillator, the output of oscillator is converted to a rail-to-rail digital output using a sine-to-square wave converter. Frequency of this square wave is measured using a frequency counter. Output of this frequency counter is multi-bit data and for practical reasons it is converted to serial data using a parallel-to-serial converter.

III. Circuit Implementation

A prototype of the complete system was implemented in a 0.18-μm BiCMOS process. The chip contains two oscillators, a BJT-based Colpitts oscillator and an inverter-based oscillator, a sine-to-square wave converter, a digital frequency counter, and a parallel-to-serial data conversion block.

A. Oscillator design

Two oscillators were designed to test their performance separately and also with the feature of selecting any one of them to interface with the complete system.

1) BJT-Colpitts oscillator: A single BJT amplifier based Colpitts oscillator was designed. BJT was chosen over MOSFET because of higher transconductance (g_m) of BJT for the same bias current. Fig. 5 presents the Colpitts oscillator interfaced with the CMUT. Resonating capacitances, i.e., C_1 and C_2 were chosen to be of same value to minimize the g_m and hence minimizing the current. The values of C_1 and C_2 were chosen such that $C_1||C_2$ cancels out the imaginary part of CMUT impedance near the parallel resonant frequency. A current based biasing scheme is used; the DC current is decided by required g_m, i.e., $I_E \approx \frac{g_m}{40}$. R_1 is chosen such that the base current flowing through R_1 gives sufficient drop to keep the base-collector junction in reverse bias mode, this ensures BJT is in forward-active (amplification) mode.

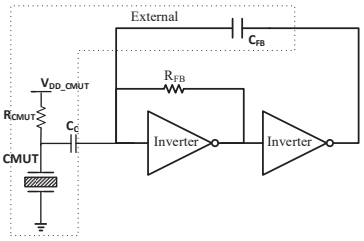

Fig. 6. Inverter based oscillator interfaced with CMUT [5].

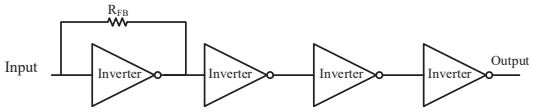

Fig. 7. Sine to square converter [5].

2) Inverter-based oscillator: For operating BJT-Colpitts oscillator at the lowest power level C_1 and C_2 needs to be varied for different resonator impedance profiles. Also the minimum current is limited by the g_m required to maintain oscillation. For these reasons an amplifier based topology was also designed for this prototype. The self-biased inverter scheme was used as the amplifier for this topology. Fig. 6 shows the inverter amplifier based oscillator interfaced with the CMUT. In this circuit R_{FB} is used to bias the inverter in the on-off transition region, where gain is maximum. The resistive feedback (R_{FB}) makes the inverter a self biased topology and will adapt to process, voltage, and temperature (PVT) variations. The external capacitor (C_{FB}) is used to reduce the gain at lower frequencies.

B. Sine-to-square wave converter

The output of the oscillator will be a sinusoidal signal, which needs to be converted to a rail-to-rail square wave for interfacing with the digital frequency counter. A sine-to-square wave converter block was designed for this reason. This block consists of a series of inverters where the first inverter is biased using R_{FB} in the on-off transition region of the inverter, to achieve maximum AC gain (Fig. 7). The main advantage of using this topology is that the static power consumption depends on the amplitude of the input sinusoidal signal. If the input sinusoidal excitation is of higher amplitude then after a few inverter stages, the signal will be rail-to-rail and all the inverter stages after that will only consume dynamic power. Also for sinusoidal signals of smaller amplitude there will be less distortion in duty cycle compared with a single stage with the same gain.

C. Digital frequency counter and parallel-to-serial converter

The frequency of the rail-to-rail signal can be calculated using a digital counter counting for a specified time known as the gate-time. Error in this frequency calculation ($\pm\frac{1}{t_{gate}}$) depends on the gate-time. Generally the gate-time is selected so that the best short-term stability is achieved for the oscillators. Equation 2 shows the effect of the gate-time on the accuracy of the frequency measurement, where N is the digital count, t_{gate} is the gate-time and $Freq$ is the calculated frequency. One way of improving accuracy in the same gate-time is counting both edges of the clock. Equation 3 shows the relation between the calculated frequency, digital count value, and the gate-time for double-edge counting. Error in the frequency measurement using dual-edge count is half compared with single-edge count. For designing a dual-edge counter a typical single-edge asynchronous counter was used and the least significant-bit (LSB) was represented by CLK or $\overline{CLK}$. If during the positive edge of the gate-time control CLK is low then LSB is represented by CLK and if during the positive edge of the gate-time control CLK is high then LSB is represented by $\overline{CLK}$. At the negative edge of the gate-time control counter output is latched and transmitted serially using external read control and read clock.

$$Freq = \frac{N}{t_{gate}} \pm \frac{1}{t_{gate}} \tag{2}$$

$$Freq = \frac{N_{double-edge}}{2 \cdot t_{gate}} \pm \frac{1}{2 \cdot t_{gate}} \tag{3}$$

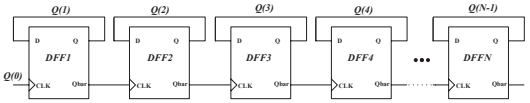

Fig. 8. Dual-edge digital frequency counter [5].

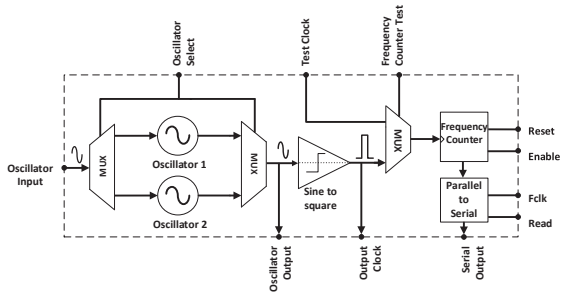

Fig. 9. Complete system designed in 0.18-μm BiCMOS process [5].

D. Complete system

Fig. 9 shows the complete end-to-end implementation of the whole system. The CMUT is interfaced to the "Oscillator input", the resonating capacitive divider is connected between "Oscillator Input", "Oscillator Output" and "Gnd". Oscillator1 (BJT Colpitts Oscillator) or Oscillator 2 (Inverter based oscillator) can be interfaced to the system using oscillator select control. Sinusoidal oscillations are converted to the digital rail-to-rail clock using a sine-to-square wave converter. Frequency of this digital clock is measured by the digital frequency counter and at the negative edge of "En" (gate-time control) the data of the frequency counter is latched. Once the frequency count value is ready "Read" (read control) is asserted and data is read in a serial manner using "F_{CLK}" (read clock).

IV. Measured Results

Fig. 10 shows a micrograph of the integrated circuit (IC) fabricated in a 0.18-μm BiCMOS process. The designed prototype IC had 16 pads to have the flexibility of testing different blocks individually. Addition of the testing feature degrades

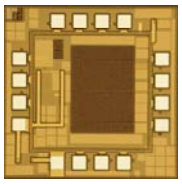

Fig. 10. Micrograph of the sensor interface IC fabricated in a 0.18-μm BiCMOS process.

TABLE I. POWER CONSUMPTION OF THE BJT-COLPITTS OSCILLATOR

	V_{DD} (V)	I_{OSC} (μ A)	$Power$ (μ W)
Nominal Vdd	1.8	172.5	310.5
Minimum Vdd	1.5	165	247.5

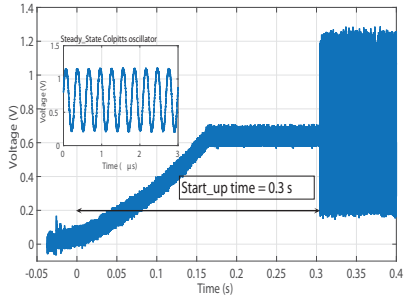

Fig. 11. Measured transient response of the BJT-Colpitts oscillator.

TABLE II. POWER CONSUMPTION OF THE INVERTER-BASED OSCILLATOR

	V_{DD} (V)	I_{OSC} (μ A)	$Power$ (μ W)
Nominal Vdd	1.8	142	256
Minimum Vdd	1.16	40	46.5

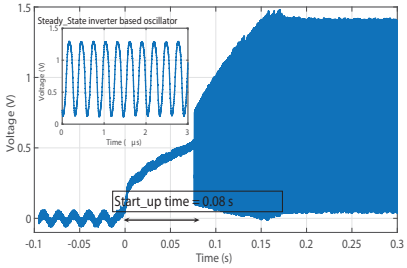

Fig. 12. Measured transient response of the inverter-based oscillator.

the performance of the complete system and individual blocks, especially oscillators, due to parasitics introduced by the pads and switches.

Oscillators were characterized separately for their nominal and minimum power consumption in continuous operation mode (Table I, II). BJT-Colpitts oscillator had a start-up time of 300 ms and steady state oscillation amplitude of 0.9 V peak-to-peak (Fig. 11). The BJT-based Colpitts oscillator had an Allan deviation of 28 Hz (3-σ) at an averaging time of 2 s. The inverter-based oscillator had a start-up time of 80 ms and steady-state oscillation amplitude of 1.2 V peak-to-peak (Fig. 12). This oscillator had an Allan deviation of 32 Hz (3-σ) at an averaging time of 0.2 s.

The digital frequency counter was also tested for its operation separately. A waveform generator (Model 33522A, Agilent Technologies, Inc., Santa Clara, CA) was used to generate an external clock of frequency 4.333333 MHz. This frequency was chosen to ensure the gate-time is not an integer multiple of the external clock. The frequency counter block was tested for gate-times from 1 ms to 1 s, shown in Table III.

TABLE III. DIGITAL FREQUENCY COUNTER MEASUREMENTS RESULTS FOR 4.333333 MHZ CLOCK

Gate-Time (ms)	Decimal Equivalent	Calculated Frequency (Hz)	Absolute Measured Error (Hz)	Max Expected Error (Hz)
0.9998240	8665	4333263	70	1000
9.9998320	86665	4333323	10	100
49.9999840	433333	4333331	2	20
99.9984400	866654	4333338	5	10
499.9998400	4333334	4333335	2	2
999.9997000	8666667	4333335	2	1

TABLE IV. COMPLETE END-TO-END SYSTEM RESULTS

Gate-Time (ms)	Decimal Equivalent	Calculated Frequency (MHz)
1.04266	7385	3.541423
10.426384	73831	3.540585
52.13184	369131	3.540360
104.26332	738078	3.539490
521.3153	3689744	3.538879
1042.6278	7378896	3.538605

Complete end-to-end performance of the system was measured for the inverter-based design at 1.8-V V_{DD}. The CMUT was biased at 13 V. The IC test board was interfaced with a microcontroller that generates the control signals. Table IV shows the frequency equivalent of the measured digital value.

V. CONCLUSION

A prototype IC for interfacing a CMUT-based resonant gas sensor is implemented in a 0.18-μm BiCMOS process. Oscillators and a digital frequency counter were studied, analyzed, designed, and tested separately for their standalone performance. A complete end-to-end system was also demonstrated wherein the integrated circuit is interfaced with a 3.6-MHz CMUT and the digital equivalent of the frequency value is read serially. With a 0.1-s start-up time, 1-s measurement time, less than 1-ms read time, and one measurement every minute the complete system's power consumption is 10 μW, when operated at 1.8-V V_{DD}.

REFERENCES

[1] H. J. Lee, K. K. Park, Ö. Oralkan, M. Kupnik, B. T. Khuri-Yakub, "A Multichannel Oscillator for a Resonant Chemical Sensor System", *IEEE Transactions on Industrial Electronics*, vol. 61, no. 10, pp. 5632-5640, Jan 2014.

[2] F. Y. Yamaner, X. Zhang, and Ö. Oralkan, "A three-mask process for fabricating vacuum sealed capacitive micromachined ultrasonic transducers using anodic bonding", *IEEE Trans. Ultrason., Ferroelect., Freq. Contr.*, vol. 62, no. 5, pp. 972-982, May 2015.

[3] M. M. Mahmud, J. Li, J. E. Lunsford, X. Zhang, F. Y. Yamaner, H. T. Nagle, and Ö. Oralkan, "A low-power gas sensor for environmental monitoring using a capacitive micromachined ultrasonic transducer", in *Proc. IEEE Sensors Conf.*, 2014, pp. 2623-2626.

[4] S. Sherrit, H. D. Wiederick, and B. K. Mukherjee, "Accurate equivalent circuits for unloaded piezoelectric resonators", in *Proc. IEEE Ultrason. Symp.*, 1997, pp. 931-935.

[5] M. Kumar, "A Low-Power Integrated Interface Circuit for a Resonant Gas Sensor Based on a Capacitive Micromachined Ultrasonic Transducer (CMUT)", Master's Thesis, North Carolina State University, Raleigh, NC, USA, 2015.